SURFACE ENGINEERING FOR APTAMER-BASED CHEMICAL SENSORS

A Thesis

by

REMINGTON P HARWELL

Submitted to the Office of Graduate and Professional Studies of
Texas A&M University
in partial fulfillment of the requirements for the degree of

MASTER OF SCIENCE

Chair of Committee,	Michael V. Pishko
Committee Members,	Mike McShane
	Victor Ugaz
Head of Department,	Anthony Guiseppi-Elie

December 2015

Major Subject: Biomedical Engineering

ABSTRACT

Bisphenol A (BPA) is a common chemical intermediate associated with adverse reproductive effects, cancer, and other human health disorders. Despite these risks, BPA continues to be employed worldwide towards the production of various plastics, resulting in widespread exposure. Recent regulations have restricted the use of BPA somewhat; however, these limitations may not be sufficient to mitigate its detrimental effects. Thus, development of a novel BPA sensor capable of rapid detection in complex biological media is paramount to adequately understand and preclude the dangers associated with BPA use.

To develop such a device, DNA aptamer probes were anchored onto a glass substrate via silanization. As a proof-of-concept, these probes were specific for a model DNA target. To achieve detection, the device was first loaded with a fluorescently-labelled version of the DNA target. This modified target could then be competitively displaced upon exposure to the native (label-free) target, which was expected to result in a loss of fluorescence corresponding to the amount of native target.

Initial results revealed that a reproducible surface for probe attachment could be achieved after 15 minutes of silanization. Probe immobilization was characterized via ellipsometry, XPS, and UV/Vis studies. These results were inconclusive; however, subsequent fluorescent target binding studies evinced reproducible binding in a quantitative manner. Moreover, minimal binding occurred in the absence of probe, implying a highly specific mechanism consistent with aptamer probe immobilization.

Thus, it is suspected that aptamer probes were reproducibly anchored onto the substrate via this method. A high concentration of reducing agent was paramount for such reproducibility, with appropriate use of blocking agents and wash buffers exerting control over sensor noise.

Subsequent competitive binding studies demonstrated the feasibility of native target detection, with a loss of fluorescence correlated with increasing native target exposure. Nevertheless, such results lacked reproducibility and did not correlate well with previous fluorescent target binding data. As a result, key areas for future research include further characterization of the probe surface and optimization of the competitive binding process to enable reproducible, sensitive detection in complex media.

DEDICATION

The following thesis is dedicated to my family, whose love and support has encouraged and motivated me throughout my education.

ACKNOWLEDGEMENTS

I would like to thank my committee chair, Dr. Pishko, and his collaborators, Dr. Coté, Dr. Kameoka, and Dr. Jackson, for their continued support and guidance in this research. I also express my gratitude towards my committee members, Dr. McShane and Dr. Ugaz, as well as Dr. Guiseppi-Elie for their guidance regarding my proposal and thesis. I likewise thank Dr. Grunlan for her assistance with my proposal. In addition, I thank Haley Marks, Javier Garza, Andrea Locke, and Brian Walton for their practical lab advice. I also thank Garrett Barker for his help as an undergraduate research assistant.

I would also like to acknowledge the financial support of the National Science Foundation and the National Institute of Health. Use of the Texas A&M University Materials Characterization Facility is likewise acknowledged. In addition, I thank Dr. Katy Kao for providing use of the GenePix microarray scanner.

Lastly, I thank my family and friends for their continued support during my time at Texas A&M.

TABLE OF CONTENTS

Page

LIST OF FIGURES

Page

LIST OF TABLES

Page

1. INTRODUCTION

1.1 Motivation

Bisphenol A (BPA) is an endocrine-disrupting chemical utilized to manufacture consumer products worldwide, with billions of pounds produced annually.[1,2] BPA is primarily employed as an intermediate for polycarbonate plastic or epoxy resin production; however, it may also be utilized directly for applications such as thermal print development. These materials are then converted into a variety of consumer products, including food storage and packaging, compact discs, dental sealants, and receipts.[2-4] As a result, exposure to BPA is widespread, affecting over 90% of the US population.[5,6]

Despite its widespread use, BPA is a known reproductive toxicant. Substantial evidence has demonstrated deleterious effects of BPA exposure on ovarian processes in both women and animal models.[7] Moreover, BPA exposure is associated with a plethora of other disorders, including cancer, cardiovascular disease, diabetes, and asthma.[4,8,9] These effects are particularly concerning regarding fetuses and neonates due to possible interference with normal development processes.[3,10]

Several techniques are employed to monitor and evaluate the extent of BPA exposure. Of these, the most common are liquid or gas chromatography followed by mass spectrometry. Through the resulting data, many regulatory agencies have estimated the risks associated with BPA exposure and established safety thresholds accordingly. However, doses below these levels have been demonstrated to adversely affect human health, even at a sub-picogram per milliliter level.[4,7] Furthermore, the extent of exposure varies widely between individuals, ranging from 0.1 to 50 ng/mL by urine analysis.[6,11]

One possible reason for this discrepancy between research and regulation is inadequate research methods. In particular, the most common technique for evaluating BPA exposure in animal models is direct administration to the stomach.[2] However, this method fails to accurately model the continual, low doses typical of human exposure.[7] Similarly, most human studies rely on concentrations of BPA and its metabolites in urine to evaluate systemic levels; however, these measurements cannot adequately determine the amount of unmetabolized (i.e., fully active) BPA in the bloodstream.[1,6] Moreover, levels of BPA in urine are often below the detection limit of conventional analytical instruments, thereby further complicating analysis.[11] Thus, there is a growing need for continuous, sensitive BPA monitoring techniques compatible with complex media such as blood.

1.2 Point-of-Care Sensors

Recent trends in biosensor development have led to significant innovation in the design of point-of-care devices. Such devices are typically designed for implementation in "near-patient" settings, such as doctor's offices. They may also be aimed at home use by patients, as in the case of some commercialized glucose monitors, or field use for applications such as environmental monitoring.[12] To be suitable for such applications, point-of-care devices require several key features. First of all, such assays must be easy to use, requiring minimal to no sample preparation and directly providing simple readouts requiring negligible training to interpret. In doing so, point-of-care devices avoid typical laboratory measurements, which often require extensive sample preparation by trained

personnel. Similarly, these point-of-care devices must be capable of rapid measurements.[12,13] This is again in contrast with current lab techniques, which commonly analyze samples over a period of days.[14] Point-of-care assays must also be low cost and portable, unlike their counterparts in laboratory settings. At the same time, point-of-care devices must maintain comparable sensitivity and reliability to traditional methods in order to yield accurate, reproducible results.[12,13]

Though the exact guidelines of what constitutes a point-of-care device vary, there are some general heuristics that define the limits for certain aspects of their design. For example, the speed of measurement (from introduction of the sample to "answer") should be sufficiently rapid to yield results in under an hour. In addition, the cost per use of the device, including consumables, should be less than $10. Likewise, the overall capital cost of the device should be less than $2000.[15]

The most common point-of-care devices used in commercial applications today are lateral flow assays.[12] These devices operate using simple fluid flows to capture target analytes and deliver qualitative results. They are cheap and easy to use; however, they suffer from low sensitivity. Thus, they are limited to applications in which the analyte is present in high concentrations and no sample preparation is required. In addition, the results given by such devices are typically in the form of a qualitative "yes/no" answer; more sophisticated measurements are difficult to achieve.[15]

Commonly, these lateral flow assays employ antibodies as a means to recognize the target analyte.[12] While suitable for many applications due to their high specificity, antibodies suffer from many drawbacks. In particular, they have limited thermal stability

and must be produced through biological means.[4,16] Moreover, antibodies designed for BPA detection are subject to considerable cross-reactivity with BPA analogues.[17] Nucleic acid aptamers have demonstrated substantial advantages over these traditional recognition elements. For example, aptamer probes exhibit much greater thermal stability than antibodies and can be chemically synthesized. In addition, aptamers are also able to maintain comparably high levels of specificity relative to traditional antibodies.[4,16,18] Furthermore, Jo et al. recently developed aptamers with very high selectivity for BPA, even when challenged with various BPA analogues.[19]

1.3 Point-of-Care Detection of BPA

There are numerous examples of point-of-care devices utilized for BPA detection in the literature. However, most of these sensors have demonstrated detection only in environmental samples such as tap water.[4,20] For instance, Xue et al. generated an aptasensor utilizing competitive binding at a gold electrode. This sensor was preloaded with DNA modified by a methylene blue redox tag to enhance the electrochemical signal. Upon exposure to BPA, this DNA target was displaced, resulting in a quantitatively decreased redox current. This mechanism enabled detection of 0.284 pg/mL of BPA in diluted tap water.[17]

Similarly, Chung et al. described a core/shell nanoparticle functionalized for BPA detection via competitive binding. In this case, Cy3-labeled probe DNA was preloaded onto complementary strands anchored to the gold surface. Introduction of BPA to this system displaced the aptamer probes from the surface, leading to a

quantitative loss of Raman signal. The limit of detection for this system was 10 fM in tap water.[21]

In contrast, Zhu et al. recently evinced an aptasensor capable of detection in fairly complex biological media. To do so, they employed a nanoporous gold film electrode functionalized with aptamer probes for electrochemical detection of BPA. This electrode directly detected BPA via its redox properties, with increasing BPA concentration leading to an increase in peak current. When evaluated using five-fold diluted serum, the lowest detected concentration was 0.5 nM BPA.[20] This study demonstrates the feasibility of BPA detection in complex media. Nevertheless, each dilution effectively lowers the concentration of BPA in the sample and ultimately limits the sensitivity of the device.[22] Thus, there is a continued need for detection of BPA in complex media with minimal dilution in order to achieve maximal sensitivity.

2. SURFACE FUNCTIONALIZATION

2.1 Silanization of Glass Substrates

For most biosensing applications, aptamers must immobilized on a solid substrate. Many such substrates are described in the literature, including glass, gold, and various polymeric matrices.[23] Of these, glass is cheap and widely available; however, in its native state, glass is relatively inert towards chemical modification.[18] Thus, immobilization of aptamer probes on glass must first begin with introduction of more reactive moieties on the surface.

To do so, glass surfaces are first cleaned using various chemical or plasma-based etching schemes.[24,25] These techniques remove contaminants, such as organic residues, and generate reactive hydroxyl moieties on the surface.[26] Generally, silanes are then employed to convert these hydroxyls into other functionalities with higher reactivity, such as amines or thiols. This process, known as silanization, is commonly performed by exposing a surface to silanes dissolved in a strong organic solvent such as toluene or acetone. Silanization must be carefully controlled to form a robust, reproducible surface. In particular, water acts as a key reagent for both the attachment and oligomerization of most silanes; thus, humidity control is imperative when generating a surface suitable for further functionalization. Such control is generally achieved by working in an inert nitrogen atmosphere.[24] Nevertheless, solution-phase silanization remains prone to multilayer island formation, particularly at lengthy incubation times.[25,27-29] Alternatively, silanization may also be carried out in the vapor phase (similar to chemical vapor deposition methods). Doing so generates more robust films approaching an ideal

monolayer; however, the vapor phase method also necessitates specialized and costly equipment (e.g., vacuum systems).[24,25]

2.2 Probe Attachment

Given the variety of substrates available, there are likewise many routes for subsequent aptamer attachment. The simplest method to do so is physisorption; however, physisorbed layers generally suffer from poor stability. Thus, most biosensors employ covalent linkages to attach aptamer probes in a more robust manner.[30] To this end, there are a variety of functional moieties that can be appended to aptamers. Of these modifications, amine and thiol terminal groups are both commercially available and frequently employed in the literature.[31] Such groups form covalent bonds via reactions with myriad other functionalities, including NHS esters and maleimides, respectively.[32] Importantly, the use of thiol moieties necessitates the addition of a reducing agent to promote probe reactivity. Although several such agents are available, most must be removed before subsequent chemistry can be performed. In contrast, tris(2-carboxyethyl)phosphine hydrochloride (TCEP) does not interfere with most subsequent functionalization steps; thus, it is often utilized as a convenient means to maintain thiolated aptamers in a reduced state throughout the sensor functionalization process.[18,33]

The detection capabilities of immobilized aptamer probes depends strongly on their surface density.[31,34] At low densities, anchored DNA adopts a "mushroom" conformation and may adsorb onto the surface.[34] This phenomenon is exacerbated by high affinity interactions between the probe and substrate, as would occur with positively-

charged substrates or gold. In either case, binding capacity is limited due to the low number of probes and unfavorable conformations.[31,34] At intermediate densities, aptamers instead enter a "crossover" conformation. In this case, probes are close enough to each other to promote conformations favoring target binding. As a result, the surface binding capacity increases substantially. At excessively high densities, however, DNA forms a "brush-like" structure, with chains extended to minimize steric hindrance.[34] This formation drastically reduces the surface binding capacity, especially for long target DNA strands.[31,34,35]

There are two primary means to control the surface density of aptamer probes. The most straightforward method is to vary the initial concentration of probe. Alternatively, the ionic strength of the immobilization buffer may utilized to modulate the charge-charge repulsion between neighboring DNA aptamers. In this case, increasing ionic strength mitigates the effects of repulsion, enabling immobilization of probes at higher densities than would occur at lower strengths.[31,34] Additionally, aptamer surface density may be affected by the underlying surface structure. For example, Shircliff et al. demonstrated that changes in the silanization process can drastically alter the number of exposed functional moieties, thereby modulating probe immobilization and subsequent density.[27]

Commercial aptamers may also include various spacer units such as oligo(thymine), oligo(ethylene glycol), or various alkyl chains.[31] These spacers improve the detection capabilities of sensors by minimizing steric hindrance of aptamers with the surface and each other. Spacers may also abate nonspecific binding (Section 3).[34] Similarly, although aptamer probes may be directly immobilized onto certain surfaces, it

is quite common to anchor aptamers by using bifunctional linker molecules. Doing so again ameliorates sensor performance by diminishing steric hindrance and inhibiting nonspecific binding.[18]

To enhance the throughput of sensing measurements, aptamer probes are commonly patterned onto surfaces so as to allow parallel experiments on the same device. A simple method for doing so is to attach modules that divide the slide into multiple wells.[36] Alternatively, high-density DNA microarrays may be formed using techniques such as automated microjet printing. These microarrays exhibit drastic improvements in throughput and reduce human error; however, they also require additional equipment to produce and can complicate subsequent analysis.[37,38]

2.3 Probe Characterization

There are several methods available to characterize the immobilization of aptamer probes on surfaces. Of these, fluorescence and radiometry techniques are the most common.[27] Fluorescent methods are relatively straightforward and simple to measure with fluorescent scanners.[39] For example, Walter et al. utilized a Sybr Green II stain to fluorescently label aptamers attached to a surface, allowing quantification of relative surface density.[35] Likewise, Elhadj et al. utilized commercially available Cy5-labelled DNA probes to similar effect.[40] However, parameters such as quantum yield and the labelling process may affect fluorescent signals, complicating subsequent quantification of data.[39] Moreover, only relative measurements may be obtained in this manner. In contrast, radiolabeling of DNA by ^{32}P yields absolute measurements of the DNA

concentration by analysis with liquid scintillation counters.[27] However, its use is associated with significant radiation hazards.[41]

An alternative to these methods is ellipsometry. This method utilizes optical measurements to detect changes in the refractive index of a material, as would occur upon binding of additional material. These variations in index are then translated into film thicknesses through optical models. For example, Elhadj et al. developed a Lorentz model for quantification of DNA binding on silicon wafers.[40] However, such quantification is highly dependent on the particular optical model.[42] In addition, differentiation between separate layers requires sufficient optical contrast (i.e., difference in refractive index), rendering this method inappropriate for certain systems.[28]

Another technique for surface characterization of immobilized probes is x-ray photoelectron spectroscopy (XPS). XPS provides quantitative data on the elemental composition of the first 2-10 nm of a surface with detection limits as low as nanograms per square centimeter.[27,39] Evaluation of DNA probe coverage generally proceeds with selection of an element unique to the probe (i.e., not found within the substrate). For instance, several groups have obtained such data by evaluating phosphorus content.[39,43] In addition, Lee et al. evinced that such data correlated well with analogous data from traditional radiolabeling.[39] However, XPS requires ultra-high vacuum conditions for operation.[42]

3. NONSPECIFIC ADSORPTION

Although sensitivity to a particular analyte is paramount to development of medically relevant biosensors, such sensitivity is often obscured by nonspecific adsorption of other particulates onto the sensor surface.[22] This phenomenon occurs largely as a consequence of surface chemistry, which can facilitate a variety of interactions with the diverse components of the detection media. Once these interactions occur, they can generate false signals or obscure specific binding sites, preventing access of the analyte to the surface.[44] Thus, nonspecific adsorption generally increases the background noise of a sensor, negatively impacting the signal-to-noise ratio and ultimately the limit of detection for target analyte.[22,45]

3.1 Factors Affecting Nonspecific Adsorption

Nonspecific adsorption occurs for a variety of reasons dependent on the particular surface as well as the detection media. For example, defects in the initial substrate, including grain boundaries and surface roughness, can contribute to incomplete coverage by the sensing chemistry, leaving raw substrate or intermediate ligands exposed to the detection media. Since most substrates and many ligands are hydrophobic, this can greatly facilitate the adsorption of hydrophobic or amphipathic solutes onto the surface.[44,45] Likewise, if probe molecules only cover a portion of the sensor surface, intermediate ligands may remain exposed, again promoting nonspecific adsorption.[44,46]

Detection media also plays a key role in nonspecific binding. Many sensors exhibit excellent performance in buffer solutions; however, when exposed to complex media such

as blood serum or cell lysates, sensor performance is considerably compromised.[47] This phenomenon occurs as a result of thousands of potential interferents present in such media.[45] Of these interferents, proteins tend to be most problematic due to their high concentrations (60-80 g/L in human blood serum), amphiphilic nature, and metastable conformations.[45,48,49] As amphiphiles, proteins display both hydrophilic and hydrophobic regions along their structures, enabling them to interact with a variety of surfaces. Additionally, proteins in blood assume a conformation in which only hydrophilic regions are in contact with the aqueous media; however, this state resides in a very shallow thermodynamic minimum of only a few kcal/mol. Thus, this native state is easily disrupted, enabling very high conformational mobility of proteins. The combination of amphiphilicity and metastability render proteins highly surface active.[45]

As a result of this high surface activity, proteins approaching a surface tend to unfold from their native conformations and adsorb onto the exposed surface. This is particularly true for hydrophobic surfaces, in which adsorption is thermodynamically favored due to the introduction of numerous hydrophobic interactions. Regardless of hydrophobicity, however, most surfaces are vulnerable to protein adsorption due to protein transport effects. Since proteins generally diffuse slowly, those that approach a surface have substantial time in which to assume a new conformational state dictated by said surface. These shifts, promoted by the release of solvating water molecules and subsequent increase in entropy, can facilitate time-dependent adsorption on surfaces that is largely independent of the surface chemistry. Furthermore, any protein adsorption that occurs tends to be highly irreversible, even if only through physical means.[45]

To counter this phenomenon, the general strategy prevalent throughout the literature has been to increase surface hydrophilicity through the use of blocking agents and hydrophilic polymers.[46,49,50] Doing so can reduce the surface energy of the sensor in aqueous media, thereby decreasing the driving force (i.e., change in Gibbs free energy) for solute adsorption. This has been demonstrated empirically, as increasing hydrophilicity is generally correlated with decreased nonspecific binding.[45]

3.2 Blocking Agents

One of the most prevalent means of decreasing nonspecific adsorption has been the use of blocking agents. This is particularly true of various immunoblotting techniques, including Western blots and ELISA. Blocking agents are designed to occupy vacant sites on the surface with molecules that do not interfere with probe specific binding mechanisms. However, due to the complexity of sensing chemistries and a dearth of understanding regarding agent adsorption, appropriate blocking agents for a given system must be determined empirically.[51]

Ideally, blocking agents should be inert towards most components of the system. Namely, they should not promote binding of any interferents present in the detection media nor impede probe-target interactions.[51,52] For instance, blocking agents should be chosen such that their size does not conceal the probe from the analyte.[52] In addition, blocking agents should have sufficient diversity of surface properties to block any moiety of the substrate that could potentially host nonspecific adsorbates.[51]

Although blocking agents can be highly effective in reducing background noise due to nonspecific interactions, they also suffer from several drawbacks. For many protein-based agents, natural variability in source materials can negatively impact reliability and performance.[51] In addition, blocking may be overly effective, producing false negatives by blocking target-probe interactions.[52] It is also possible that blocking agents may become detached from the surface, form multilayers with proteins present in the detection media, or simply produce an intrinsic signal.[44,53] In each of these cases, a false positive signal would be generated.

Protein-Based Blocking Agents

Common blocking agents include proteins and non-ionic detergents. Protein agents have the advantage of permanently blocking vacant sites on the sensor surface; thus, they only need to be added to the surface once (generally after probe attachment). These agents may, however, be added again in subsequent steps to further reduce nonspecific binding. Additionally, protein blocking agents tend to provide added spacing and stability for probes.[51]

There are many examples of protein-based blocking agents throughout the literature. One of the most prevalent is bovine serum albumin (BSA). BSA is a globular protein with dimensions 140 x 40 x 40 $Å^3$ that is negatively charged at neutral pH (pI 4.7). It is inexpensive and stable either dry at room temperature or in solution at 4° C. In addition, BSA does not interfere with most biochemical interactions, including DNA hybridization.[51,54,55] Typically, a BSA solution with concentration of one to three percent

is employed to achieve optimal blocking of nonspecific interactions. BSA does, however, suffer from lot-to-lot variability related to fatty acid impurities.[51] Also, as a single protein, BSA lacks the diversity to adequately block surfaces with highly varied surface moieties.[51,56]

An alternative to BSA is casein derived from non-fat dry milk. Like BSA, casein is negatively charged at neutral pH (pI 4.6). Unlike BSA, however, casein typically forms large, spherical micelle structures with calcium phosphate nanoparticles. These structures commonly approach 1000 Å in diameter. In addition, casein is generally insoluble in aqueous media, often necessitating the use of slightly alkaline buffers. Unfortunately, this issue can render casein solutions very viscous and difficult to remove from certain surfaces, marring sensor reproducibility.[54] Despite these issues, casein is frequently employed as the primary blocking agent in DNA blots.[51]

Another example of a protein blocking agent is non-fat dry milk (NFDM). The proteins present in this mixture typically consist of approximately 80% casein (again incorporated into micelles) and 20% whey (with carbohydrate lactose). Since whey and carbohydrate lactose do not form larger structures as casein does, NFDM has a much more diverse size distribution than casein alone.[54] In addition, NFDM is much more soluble in aqueous media than pure casein.[51] Thus, it is widely applicable to many sensor systems. However, possible histone contaminants may interfere with assays designed to interact with DNA.[51]

A fourth blocking agent is normal whole sera. Sera are considered among the most effective blocking agents due to their extensive molecular diversity. Such diversity not

only blocks all manner of nonspecific interactions, but also maintains bioactivity of certain probe molecules. Thus, it is commonly recommended for applications encountering very difficult blocking issues. However, the use of sera may be limited by cross-reactivity with many protein-based probes (e.g., anti-IgG antibodies).[51]

Detergent-Based Blocking Agents

An alternative class of blocking agents is detergents. Generally, non-ionic detergents are employed so as to provide sufficient blocking while precluding any deleterious interactions with various plastics. Unlike their protein-based counterparts, detergents serve as temporary blocking agents. They can be removed simply by washing the system; thus, they must be incorporated in all buffers in order to be effective. Detergents also often necessitate the use of high concentrations (above the critical micelle concentration) for sufficient blocking. Fortunately, such detergents are inexpensive. Additionally, they are stable in wash buffers for extended periods. Thus, they are often utilized during wash steps for blocking any areas of the sensor that may become exposed when other molecules are removed. Detergents are also effective at removing any molecules that may become physically trapped at the corners of a well or other barrier. For these reasons, detergents are often utilized in combination with protein blocking agents to provide complementary blocking capabilities. Tween 20 is the most common detergent utilized due to its wide applicability. Triton X-100 is also effective, but it is prone to disrupting desired specific interactions. Thus, its use should be limited to low concentrations.[51]

3.3 Capping Agents

A similar method to the use of blocking agents is that of capping agents to passivate a functionalized surface. Such agents are designed to react with any residual functional moieties remaining after probe immobilization. In doing so, any additional surface reactions that could promote nonspecific adsorption can be minimized.[46] Common examples of capping agents include ethanolamine, 2-(2-aminoethoxy)ethanol, and succinic anhydride. These agents may also introduce additional functionalities for probe immobilization or modify surface properties to support probe bioactivity.[35,46] However, it is often difficult to inactivate all surface functional groups. Furthermore, the use of capping agents introduces an additional synthetic step, which in turn can lead to additional losses, inefficiencies, and side reactions.[46]

3.4 Polymers

The other major method for reducing nonspecific adsorption is the use of polymers. Generally, these polymers are hydrophilic in nature.[46] As a result, they form a hydration barrier in aqueous solution due to the presence of bound water molecules.[47,57,58] This barrier serves to minimize nonspecific adsorption due to the high enthalpy required to remove the attached water molecules.[47] The aqueous barrier can also maintain the bioactivity of any attached probes.[46] In addition, many polymers have very high conformational mobility.[59] Such flexibility provides steric hindrance, thereby minimizing nonspecific adsorption via high conformational entropy.[57,59]

The degree to which hydration and flexibility affect nonspecific adsorption and bioactivity is determined in part by polymer length.[46,47] Since prevention of nonspecific adsorption and support of probe function often counteract each other, there is generally some optimal length at which sufficient characteristics are achieved.[46] Polymer density can likewise have a tremendous impact on sensor performance. In particular, if polymer density is low, the surface vacant sites may not be adequately protected from approaching interferents.[45]

3.5 Polymerization Methods

One key parameter for determining polymer density is the mode of polymer immobilization. Many biosensing platforms utilize preformed polymer chains that can be "grafted to" the surface of the sensor via some functional end group. These polymers then can form self-assembled monolayers (SAMs) on the surface, thereby shielding the underlying substrate from potential interferents.[45] Such polymers are commonly added to the substrate along with a different polymer designed to allow facile probe immobilization, yielding a mixed SAM bearing both properties.[60] For example, alkanethiols are often combined with low fouling poly(ethylene glycol) derivatives to counteract their inherent vulnerability towards nonspecific adsorption.[58,60] Density of such SAMs can be controlled primarily by incubation time, with longer incubations increasing saturation of the surface. Increasing density of SAM polymers on the surface has been correlated with decreased nonspecific adsorption for the reasons discussed previously.[44] However, there is a limit to the density that can be achieved using the "grafting to" method.[46] When preformed

polymers are anchored to the surface, they generate significant steric hindrance that inhibits anchoring of any other polymers in their vicinity. Thus, sufficient protection from nonspecific adsorption in complex media with this method alone has yet to be realized.[45]

To remedy these issues, recent research has instead focused on surface-initiated polymerization methods.[46,61] In these techniques, polymer chains are "grafted from" the solution phase by immobilizing an initiator species onto the surface. This initiator species is then used to grow a polymer chain directly from the surface using monomers present in the solution. Since these monomers are much less bulky than a preformed polymer, they exhibit much less steric hindrance.[45] As a result, polymer chains can grow much more densely than could be achieved via "grafting to" techniques.[45,46] In fact, polymers can be grown so densely that they assume an extended polymer "brush" structure.[45-47,58] These polymer brushes have demonstrated significantly improved resistance to nonspecific adsorption relative to polymers exhibiting the low-density "mushroom" architecture characteristic of other techniques.[45,47,58] However, such polymerization systems often employ complicated synthetic procedures and require materials that are not commercially available.[45,62]

3.6 Wash Steps

Nonspecific adsorption can also be affected drastically by the wash procedure employed to remove adsorbates.[38,45] Although such washes are simple in principle, they often act as significant sources of variability. There are many parameters related to washing that must be optimized in order to provide reliable results. In particular, the

choice of wash buffer can have a tremendous impact on the amount of adsorbates remaining on the sensor surface. Generally, such buffers should include a low concentration of non-ionic detergent (below its critical micelle concentration) so as to remove any physically trapped interferents while avoiding disruption of any desired specific interactions. The chosen buffer should also be physiologically compatible so as to maintain probe bioactivity. Delivery and removal of the wash buffer must also be optimized. Both should be gentle enough to prevent loss of specific interactions. Additionally, removal should not dry out the sensor surface, especially when employing protein-based probes. Rather, a consistent amount of residual liquid should remain on the sensor surface to increase reproducibility. To adequately remove any nonspecific adsorbates while leaving specific interactions intact, three to five wash steps are typically necessary. A final soak in the wash buffer can serve to remove most residual liquid, especially liquid trapped in the corners of wells and other features.[63]

4. METHODS

Given the need for a versatile sensing surface for BPA detection, DNA aptamer probes were immobilized on glass substrates. To ascertain the reliability and accuracy of such sensors, a proof-of-concept design was employed with probes specific for a model DNA target. Detection was achieved through competitive binding, in which preloaded fluorescently-labeled targets were displaced upon exposure to the native (label-free) target (Figure 1). Surface characterization and evaluation of sensor performance were conducted using a variety of techniques, including XPS, ellipsometry, UV/Vis measurements, and fluorescent imaging.

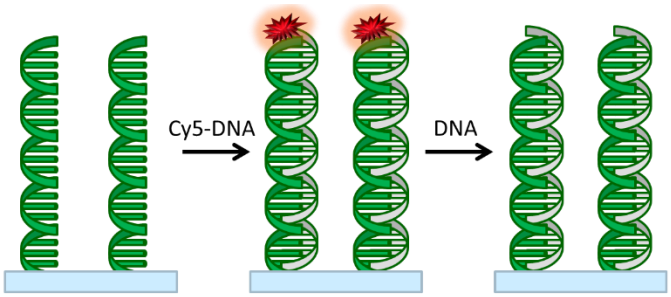

Figure 1. Immobilization of aptamer probes onto glass enables capture of fluorescent DNA targets. Subsequent exposure to label-free target leads to a loss of fluorescence due to competitive binding.

4.1 Materials

Potassium phosphate monobasic, sodium hydroxide, and methanol were purchased from Fisher Scientific. Sodium phosphate dibasic, sodium phosphate monobasic,

hydrochloric acid (37%), bovine serum albumin (BSA), sodium citrate, silicon wafers, and molecular sieves (3 Å beads, 8-12 mesh) were purchased from Sigma-Aldrich. Tris(2-carboxyethyl)phosphine hydrochloride (TCEP), magnesium chloride, and sodium dodecyl sulfate (SDS) were purchased from Amresco. Sodium chloride, ethylenediaminetetraacetic acid (EDTA, 0.05 M), and dimethylsulfoxide (DMSO) were purchased from BDH. Tween 20 and concentrated sulfuric acid were purchased from Acros Organics. Toluene, (3-aminopropyl)trimethoxysilane (APTMS, 97%), and (3-acryloyloxypropyl)trimethoxysilane (AcPTMS, 95%) were purchased from Alfa Aesar. Research-grade skim milk powder (i.e., non-fat dry milk) and casein were purchased from MP. Maleimide-PEG_2-succinimidyl ester ($SM(PEG)_2$) was purchased from Quanta Biodesign. PEG_{5000}-silane was purchased from Creative PEGworks. HPLC-purified DNA probes and targets were purchased from IDT and Eurofins (Appendix A.2). Slide modules and gaskets were purchased from Grace Bio. Desi-Vac storage boxes were purchased from VWR.

Fluorescent images were obtained using an Axon Instruments GenePix Personal 4100A microarray scanner. A J.A. Woollam Alpha-SE ellipsometer with CompleteEASE software was employed for ellipsometry measurements. XPS measurements were acquired via an Omicron XPS/UPS system with Argus detector. Microplate UV/Vis readings were obtained using a Tecan Infinite M200 Pro and a Tecan Nanoquant plate.

4.2 Silanization

Slides were cleaned and activated using a two-step process adapted from Cras et al.[26] To do so, two slides were submerged in freshly prepared 1:1 (v/v) methanol/hydrochloric acid solution for thirty minutes. Afterwards, these slides were rinsed with approximately 40 mL of water and dried using a stream of nitrogen. This rinsing process was repeated again if schlieren lines were still present on the surface after drying. Next, slides were placed in concentrated sulfuric acid for thirty minutes. The sulfuric acid supernatant was subsequently removed and each slide was rinsed with approximately 40 mL of water. However, residues frequently remained on the surface after this wash; thus, a second wash utilizing approximately 40 mL of water was conducted for most slides. This wash was again followed by drying with nitrogen.

Once the slides had been cleaned, they were silanized in a manner similar to that employed by Zhou et al.[64] To begin, a nitrogen glovebag was connected to the nitrogen line and purged for several minutes. Meanwhile, a silanization solution consisting of 0.1% (v/v) APTMS in toluene was prepared and stirred for two minutes to promote optimal mixing. This solution also contained 0.1% (v/v) AcPTMS for preliminary silanization studies or 10:1 mol PEG_{5000}-silane/mol APTMS for PEG blocking studies. Slides were then immediately exposed to this solution and placed inside the glovebag. The glovebag was subsequently sealed for either 15, 30, 60, or 300 minutes with no additional nitrogen influx. After this incubation period, slides were removed, then promptly rinsed with fresh toluene and again dried with nitrogen. For preliminary optimization studies, these slides were subsequently heated in an oven at approximately 100 °C for two hours before

storage. In most other experiments, they were instead directly stored in plastic Petri dishes, sealed with Parafilm, and placed in a vacuum box for two days.

4.3 Aptamer Probe Immobilization

Once silanization was complete, aptamer probes were immobilized onto the glass surface (Figure 2). In most studies, 16-well slide modules were attached onto the silanized slides. The remainder of the procedure varied considerably depending on the particular experimental conditions being evaluated. For most slides, each well was exposed to 75 µL of 10 mM $SM(PEG)_2$ in PBS+ (PBS, 5 mM $MgCl_2$, 1% (v/v) Tween 20; Appendix A.1). Negative control wells were filled with PBS+ alone. These slides were then covered with Parafilm and placed in Petri dishes humidified via wet paper towels and sealed with Parafilm. The slides were then shaken on a rocker at a 15° tilt angle for one hour.

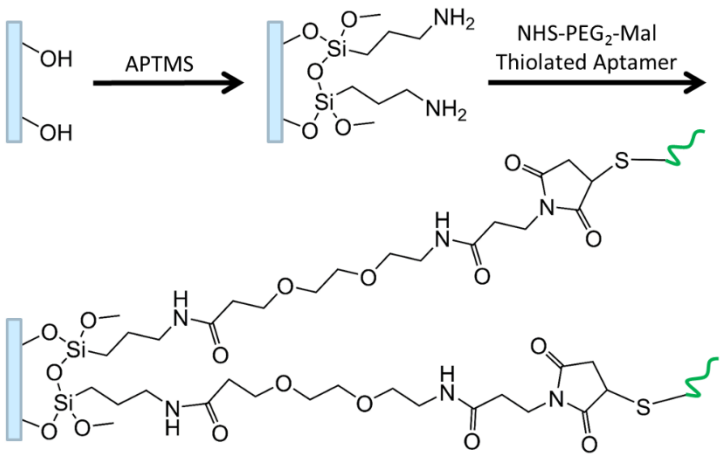

Figure 2. Immobilization of aptamer probes onto a glass surface prepared through silanization and exposure to a bifunctional linker. Aptamers not to scale.

During this time, the working probe solution was freshly prepared. For high TCEP variants, a 40 mM solution of TCEP in PBS+ was freshly prepared. Otherwise, stock 10 mM TCEP neutralized with sodium hydroxide was utilized. In both cases, aptamer probe was diluted in PBS+ and heated to 85-90 °C for 150 seconds. After cooling for approximately five minutes, TCEP solution was added to the probe solution such that the final concentration of TCEP was 10 mM or 100 μM, respectively. The final probe concentration for most experiments was 1 μM. This probe solution was then incubated for thirty minutes to ensure sufficient reduction of the thiol moieties.

Once the slides had been exposed to $SM(PEG)_2$ linker for an hour, supernatants from each well were removed and discarded using a multichannel pipette. These wells were then washed with 112.6 μL of ultrapure water per well by pipetting back and forth ten times. Afterwards, supernatants were again discarded and the wells were dried with nitrogen. Next, wells were exposed to the working probe solution for two hours and placed on the rocker as before. In the case of negative controls, probe solution was again substituted for PBS+. Subsequent washing and drying proceeded as with the $SM(PEG)_2$ incubation except that 10-20 μL of each supernatant was stored when necessary for UV/Vis measurements.

After immobilizing aptamer probes on the surface, nonspecific interactions were inhibited using blocking agents such as non-fat dry milk, bovine serum albumin, and casein. These blocking agents were freshly prepared at certain concentrations in order to evaluate their effectiveness (Table 1). In each case, the chosen blocking agent was added to the slide wells and allowed to incubate for two hours on the rocker. Following this

incubation, slides were rinsed as before (without drying). Up to 50 μL of water was then added to each well and paper towels were rewetted to reduce evaporation during overnight storage in the vacuum box.

Table 1. Blocking agent type and evaluated concentrations.

Blocking Agent	Concentration (mg/mL H_2O)
Milk	100
	10
	1
BSA	20
	2
	0.2
Casein	20
PEG_{5000}-silane + BSA	10:1 mol PEG/mol APTMS + 20 mg BSA/mL H_2O

Table 2. Wash buffer composition, order, and incubation time.

Wash	Composition	Time (min)
I	2x SSC, 0.2% SDS, 42 °C	5-10
II	1x SSC	5-10
III, IV	0.2x SSC	2

4.4 Fluorescent Preloading and Detection of Native Target

The following day, Cy5-DNA solutions were freshly prepared by dilution with 6x SSPE. These solutions were covered with aluminum foil until use to minimize photobleaching. Next, each well was rinsed (without drying) as before. Afterwards, slides

were exposed to Cy5-DNA at various concentrations, with PBS+ or 6x SSPE serving as negative controls. Fresh paper towels were put into place and the Petri dishes were covered with aluminum foil to prevent photobleaching before placing the slides on the rocker for two hours.

Meanwhile, various wash buffers were prepared according to Table 2.[65] Once the Cy5-DNA incubation was complete, supernatants were discarded as before. The slides were then washed using water (for preliminary studies) or 75-100 μL of each wash and placed on an orbital shaker. After all washes were complete, slides were either exposed to native DNA target or dried and stored in the vacuum box for subsequent fluorescence measurements.

Detection of native DNA target proceeded similarly to initial preloading with Cy5-DNA. In this case, preloaded slides were exposed to various concentrations of native target immediately following the previous rinse steps. PBS+ and 6x SSPE were again utilized for negative controls. This incubation proceeded on the rocker for either two hours or overnight. Following this period, wash buffers were prepared as for the preloading step and utilized as before. Slides were then dried and stored in the vacuum box for subsequent fluorescence measurements.

4.5 Slide Characterization

Fluorescent Imaging

To obtain fluorescence data, slides were imaged using a GenePix microarray scanner with an excitation wavelength of 635 nm. Photomultiplier tube (PMT) gains were

varied based on initial preview scans in the Cy5 channel; generally, these ranged from 400-700. Contrast and brightness were adjusted using the native scanner software (Acuity) as well as ImageJ to improve image visibility without affecting underlying data. ImageJ was then utilized to quantify data from each well. These data were further analyzed using Microsoft Excel (Appendix A.3).

Verifying Probe Immobilization

Several techniques were employed to evaluate probe anchoring to the surface. For example, aptamer probes modified with Cy5 were anchored onto the glass surface instead of their non-fluorescent counterparts. These Cy5 probes were protected from photobleaching by covering slides with aluminum foil during incubation. Slides modified in this manner were subsequently stored in a vacuum box and imaged using a fluorescent microarray scanner as before.

In addition, ellipsometry was utilized to determine the thickness of the probe layer on the surface. However, because this probe layer has very similar optical properties compared to the underlying glass substrate, initial results were inconclusive. Thus, silicon wafers were employed as an alternative substrate capable of providing sufficient optical contrast for reliable measurements. Since silicon shares very similar surface chemistry with glass, silanization and subsequent functionalization proceeded as with previously described methods.[28,43] Despite these similarities, however, 16-well slide modules would not adhere to the silicon surface following silanization; thus, wafers were divided into small pieces. After silanization, these slides were functionalized in a humidified 16-well

plate. These silicon wafers were then analyzed using a J.A. Woollam ellipsometer from 382 to 893 nm immediately before probe immobilization and after the subsequent probe incubation, washing, and drying steps.

XPS was likewise employed to determine the phosphorous content (and thus aptamer probe content) on the glass surface. Due to size constraints of the sample chamber, slides were cut into small pieces and functionalized using a 16-well plate as with ellipsometry. Initial scans evinced that phosphorus intensity was too low to be detected via conventional settings; thus, the intensity was increased by utilizing a larger aperture and higher pass energy (up to 150 eV). However, such settings also precluded the use of high resolution scans to characterize specific bonds.[66]

To troubleshoot aptamer immobilization, probe supernatants were analyzed using a 16-well Nanoquant plate designed for DNA quantification. To do so, 2 μL of each supernatant was spotted into the wells and scanned at 260 and 280 nm using a Tecan microplate reader. These results were compared to PBS+ blanks as well as aliquots of the remaining working probe solution.

5. RESULTS AND DISCUSSION

5.1 Aptamer Immobilization

Ellipsometry was utilized to tune the initial silanization process for this particular application. Silicon wafers were silanized for 15, 30, 60, or 300 minutes according to the protocol adapted from Zhou et al.[64] Results from ellipsometry evinced that increasing the silanization time tended to increase both the thickness of the layers and the variation in these thicknesses (Figure 3). This trend was attributed to the formation of multilayer islands due to polycondensation of silanes, as evinced by the extreme variation in 300 minute thicknesses (MSE>100, CV=9.55%). Thus, to achieve the most homogenous and reproducible surface for subsequent functionalization and sensing experiments, the 15 minute silanization scheme (6.37 ± .0878 nm, MSE=3.37, CV=1.38%) was employed for future experiments. This scheme resulted in surfaces consisting of approximately 13 silane layers, assuming an ideal monolayer thickness of 5 Å.[67]

This silanization process was further refined in subsequent preloading experiments. In particular, the acryloylsilane was removed, thereby increasing the loading capacity of the surface for amine groups. As expected, this increased density of amines improved surface functionalization as evinced in subsequent Cy5 target binding studies. The oven annealing step, despite its suggested importance in the literature, was likewise removed with minimal effect.[64] Similar studies employing Piranha solution as an alternative cleaning method demonstrated negligible benefit. Thus, although Piranha is widely employed in the literature, the aforementioned acid washes were utilized instead to avoid safety issues associated with Piranha use.[26]

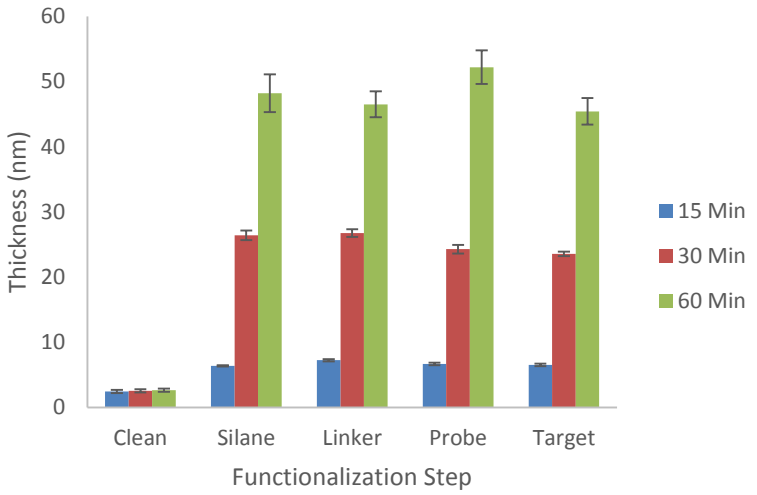

Figure 3. Optimization of silanization via ellipsometry. From left to right: Cleaned substrates, silanized, NHS-PEG-Mal, aptamer probe, DNA-Cy3. Note that some steps and reagents were not preserved in more recent procedures.

Once silanization was optimized, several techniques for probe immobilization were evaluated. To begin, probe solution was added to slides by either filling the wells or spotting 1 μL of solution onto the surface (Figure 4). This spotting method conserved expensive probes and minimized accumulation of molecules at the well walls; however, it also prevented use of the rocker to provide convection for improved reaction kinetics. Moreover, smudging effects complicated subsequent quantitative analysis. In contrast, the filling method provided complete coverage of each well, ensuring higher probe exposure and consequently higher probe anchoring. This technique also allowed use of the rocker to provide convection, thereby promoting more uniform surface coverage and simplifying analysis.

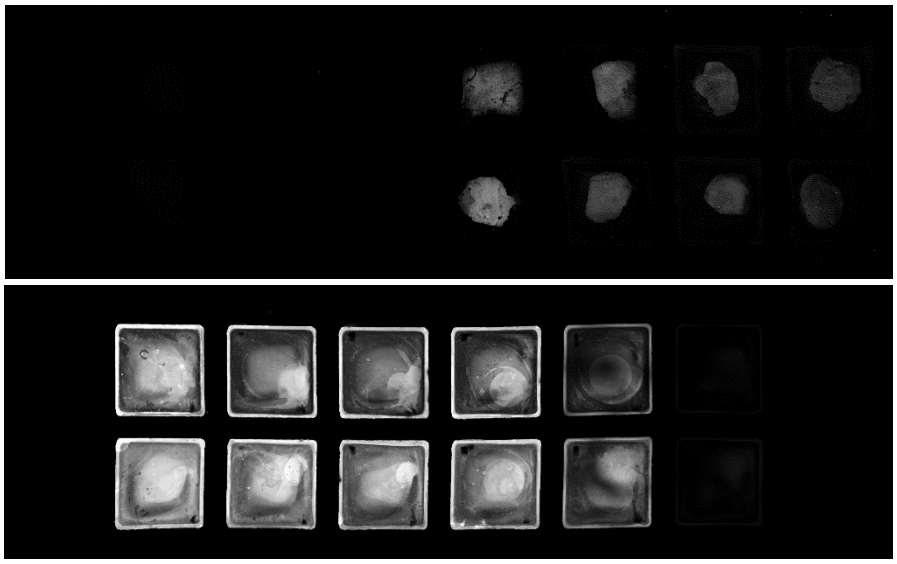

Figure 4. A comparison of spotting (top) and whole-well (bottom) probe immobilization techniques after exposure to Cy5-target. Brightness and contrast were adjusted for clarity. Note that differences in intensity stem primarily from other experimental differences (e.g., Cy5-target concentration).

A variety of methods were employed to characterize these probe-containing surfaces. The simplest of these was the preliminary immobilization of a Cy5-labeled version of the probe. Doing so evinced that probes could be anchored onto the surface; however, these initial data also demonstrated poor reproducibility with low signal. These results were substantiated by issues with downstream target binding studies.

To further characterize these surfaces, ellipsometry was again employed. In this case, silicon wafers were divided into small pieces and functionalized individually. After scanning with the ellipsometer, data were fitted using both Cauchy and Lorentz models from the literature to determine the thicknesses of the $SM(PEG)_2$ and DNA layers, respectively (Appendix A.4). These results indicated a decrease in thickness of 0.52 ±

0.027 nm (n≥3, MSE=16.0, CV=5.19%) occurred upon probe immobilization, thereby implying that probes were not anchoring onto the surface in sufficient amounts. The slight decrease in thickness could be attributed to hydrolysis of linker moieties or small portions of the underlying silane network due to prolonged exposure to aqueous solution.[25,67]

XPS was then employed to confirm these results. To do so, glass slides were similarly cut into small pieces and functionalized individually in order to fit within the small sample chamber. Slides with probe were then expected to evince a peak due to the presence of phosphorus in the DNA backbone. Initial scans evinced that the surface concentration of phosphorus was quite low; thus, both pass energy and aperture size were increased to increase intensity at the cost of resolution. Upon doing so, a small but detectable amount of phosphorus was revealed. However, this concentration varied considerably, with no clear difference between slides with probe and control slides without probe (Table 3). Coupled with previous ellipsometry results, these data indicate that probe immobilization was very poor. In addition, the phosphorus detected on the surface likely represented residual ions from PBS+ buffer or TCEP.

Table 3. XPS phosphorus content of low TCEP surfaces.

Linker	Probe	% Phosphorus	n
10 mM	1 µM	0.549	1
10 mM	10 µM	1.52	1
-	1 µM	0.731 ± 0.447	2
10 mM	-	1.46 ± 0.329	2

To remedy these issues, the concentration of TCEP added to probe solution was increased 100-fold. Since TCEP is responsible for reducing probe dithiols into reactive thiol moieties, such an increase was expected to drastically increase the amount of probe anchored via surface maleimide groups. Doing so considerably improved subsequent Cy5-target binding studies (Section 5.2); however, competitive binding studies still failed to achieve reproducibility (Section 5.3).

These concerns demanded further characterization of the surface to determine the core problem. However, previous characterization by ellipsometry and XPS proved rather cumbersome. In particular, ellipsometry provided only an indirect measure of probe immobilization via thickness on a silicon wafer. Although these wafers share similar surface chemistries with glass slides, there may be subtle differences that this technique does not address. Moreover, ellipsometry results are highly dependent on interpretation through an optical model. To my knowledge, no such model exists for the exact system employed; thus, the model utilized is an approximation that may not properly account for the properties of the two layers. Similarly, XPS results necessitated substantial deviations from typical functionalization procedures to meet the size constraints of the sample chamber. In addition, such results may be obscured by residual buffer ions or TCEP on the surface. Thus, the only element truly unique to thiolated DNA probes in the overall procedure is sulfur, which is present in concentrations below the limit of detection of the instrument.

In contrast to these methods, characterization via UV/Vis absorbance using a Nanoquant plate provides a simple, albeit indirect, means of determining probe

immobilization. Consequently, this technique was employed to characterize the surfaces exposed to high TCEP. Initial data indicated negligible difference (-1.13 ± 2.51%, n=16, $p<0.5$) between the probe supernatants and the original working probe solutions, again implying that probe anchoring was poor. Attempts to promote improved linker attachment via increased incubation time proved futile, yielding similarly high variability with little change in probe immobilization. These results were attributed to hydrolysis of the linker moieties upon prolonged exposure to aqueous solutions. To avoid any issues with silanization and linker anchoring, commercially available maleimide slides were employed. However, these results were again similar to initial results and evinced very poor probe attachment.

Upon further analysis of these results, however, it would appear that the Nanoquant data is inconclusive. Such UV absorbance measurements are typically verified by the ratio of absorbances at 260 and 280 nm, with pure DNA expected to evince ratios between 1.8 to 2.0.[68] However, initial results demonstrated a ratio of 1.60 ± 0.057 (n=16, CV=3.59%, $p<0.01$), thereby indicating significant interference. Given that these measurements were blanked with pure PBS+, the only additional compound other than DNA should be TCEP, which is present in significantly higher amounts (10 mM). Although TCEP is generally not considered an interferent in UV/Vis measurements of DNA concentration due to its low absorbance at 260 and 280 nm, the comparatively high amount (10,000-fold higher molar concentration) likely contributed substantial absorbance to each measurement, preventing accurate measurement of probe immobilization via this method. Nevertheless, repeating the initial experiment with fresh $SM(PEG)_2$ stock indicated no significant

difference between the expected and observed ratios (n=13, CV=10.1%, $p<0.05$). Consequently, characterization and quantification of the probe immobilization process remains a key area for future research.

5.2 Fluorescent Target Preloading

To assess the capacity of sensor surfaces to capture fluorescent targets for sensor preloading, probe-functionalized glass slides were exposed to a Cy3-labeled DNA target complementary to the anchored probe. These initial data indicated strong fluorescence, even in the absence of probe. This nonspecific binding likely occurred via physisorption of the target DNA molecules during prolonged incubation.

As a result, several blocking agents were evaluated to determine their ability to block nonspecific interactions without causing significant interference to desired target-probe interactions. In particular, NFDM, BSA, and casein were employed at various concentrations between the probe and target incubations. A PEGylated silane was similarly introduced during silanization along with the aminosilane necessary for probe attachment. Since many of these agents are proteins that exhibit autofluorescence at the excitation wavelength of Cy3, a Cy5-labeled DNA target was employed for these and all subsequent experiments.

Despite these blocking steps, however, initial results with NFDM indicated that substantial nonspecific binding continued to obscure measurements. Consequently, the stringency of target wash steps was increased to minimize any remaining physisorbed species on the surface. To do so, the initial water wash was replaced by a series of SSC

washes with added convection from the orbital shaker. Doing so greatly reduced the noise in fluorescent images while maintaining relatively high signal. These results were attributed to improved removal of nonspecifically-bound Cy5-targets with minimal effect on the stronger probe-target interactions. This stringency would later be further increased by utilizing higher wash volumes and introducing additional convection by repeated pipetting. As before, this increased stringency further reduced the noise with negligible detriment to the signal.

Once the sensor noise had been substantially reduced, other parameters were likewise varied in order to boost the signal inherent in the probe-target binding process. In particular, SSPE was utilized as an alternative to PBS+ for DNA-DNA hybridization. Upon doing so, surfaces exhibited substantially improved fluorescence trends, thereby indicating a greater number of binding events.

After implementing these improvements, each of the aforementioned blocking agents was then evaluated for its blocking capabilities. Of these agents, casein proved least effective due to low solubility in aqueous solutions (Figure 5). Such poor solubility would likely render accurate and reproducible usage difficult, as reflected in the high noise level upon agitation. Similarly, the PEG-silane exhibited poor solubility at the tested concentration. Unlike casein, this compound was quite effective in reducing noise; however, it also reduced the fluorescent signal substantially compared to other methods despite being measured at increased gain. Thus, its use was rejected in order to preclude the need for significant optimization and avoid compounding existing issues with low signal.

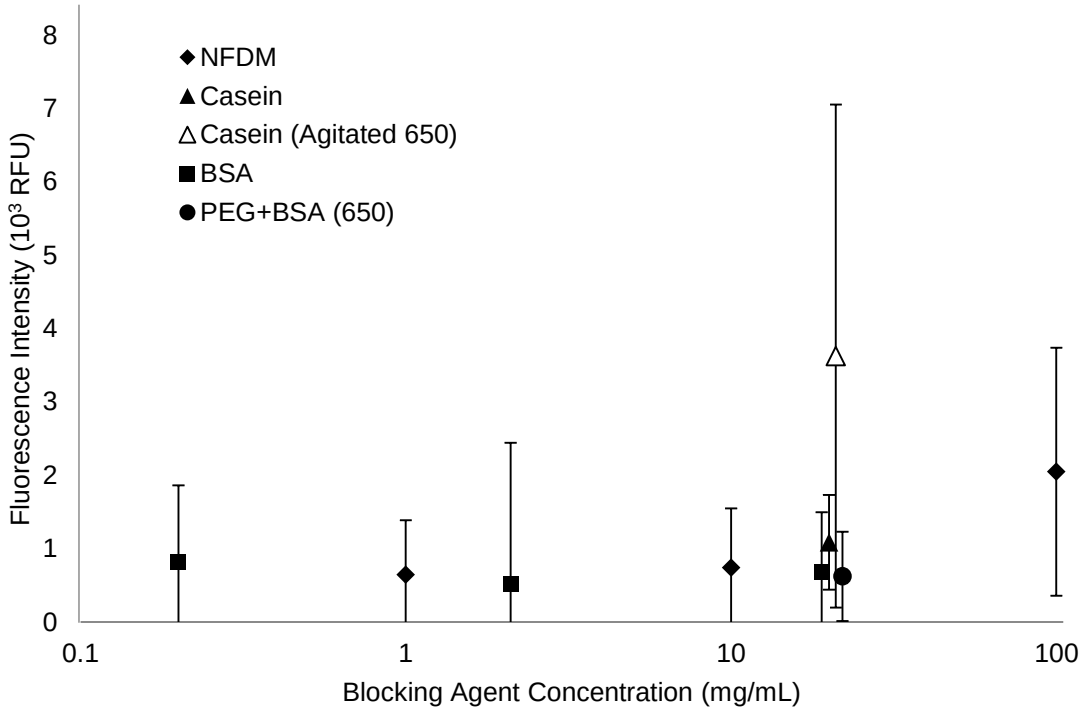

Figure 5. Comparison of blocking agents at various concentrations on low TCEP substrates. 10 mol PEG_{5000}-silane/mol APTMS was employed for PEG+BSA measurements. Casein and PEG_{5000} concentrations were determined without accounting for undissolved material and are thus lower than indicated. PMT gains were set at 550 for all data except agitated casein and PEG+BSA, which were at 650. For NFDM and BSA, n=1. For all others, n=3. Error bars indicate standard deviations. Data at 2 and 20 mg/mL are spaced slightly apart for clarity.

In contrast, NFDM and BSA both exhibited sufficient noise reduction while maintaining adequate signal at various concentrations. Of these, NFDM was initially chosen due to its low cost. However, experiments with NFDM on low TCEP substrates repeatedly demonstrated poor reproducibility. Thus, BSA at the highest tested concentration (20 mg/mL water) was employed as an alternative.

Despite these gains, however, the reproducibility of Cy5-target capture remained low, as demonstrated by high variations in the fluorescent signal between experiments. After significant probe immobilization studies, it was determined that the root cause of this phenomenon was actually poor reproducibility of probe attachment. Thus, when probes were anchored onto the surfaces by employing high levels of TCEP, the resulting sensors exhibited drastic improvements in both fluorescent signal and reproducibility upon Cy5-target capture (Figure 6). These results demonstrate the feasibility of Cy5-target loading in a quantitative manner, with higher levels of reproducibility likely achievable through further optimization. Moreover, very low signal is detected in control wells lacking probe, indicating minimal nonspecific binding. Nevertheless, the reproducibility between different slides is not as clear; thus, these sensors would likely need to employ calibration via an external standard in order to provide precise results.

This drastic amelioration of fluorescent signal would seem to indicate vastly improved probe immobilization, thereby enabling greater capacity for target binding. This notion is supported by control results that indicate low background in absence of probe, implying a highly specific binding mechanism. Given the inconclusive evidence regarding probe immobilization, however, it remains difficult to validate this claim without further investigation.

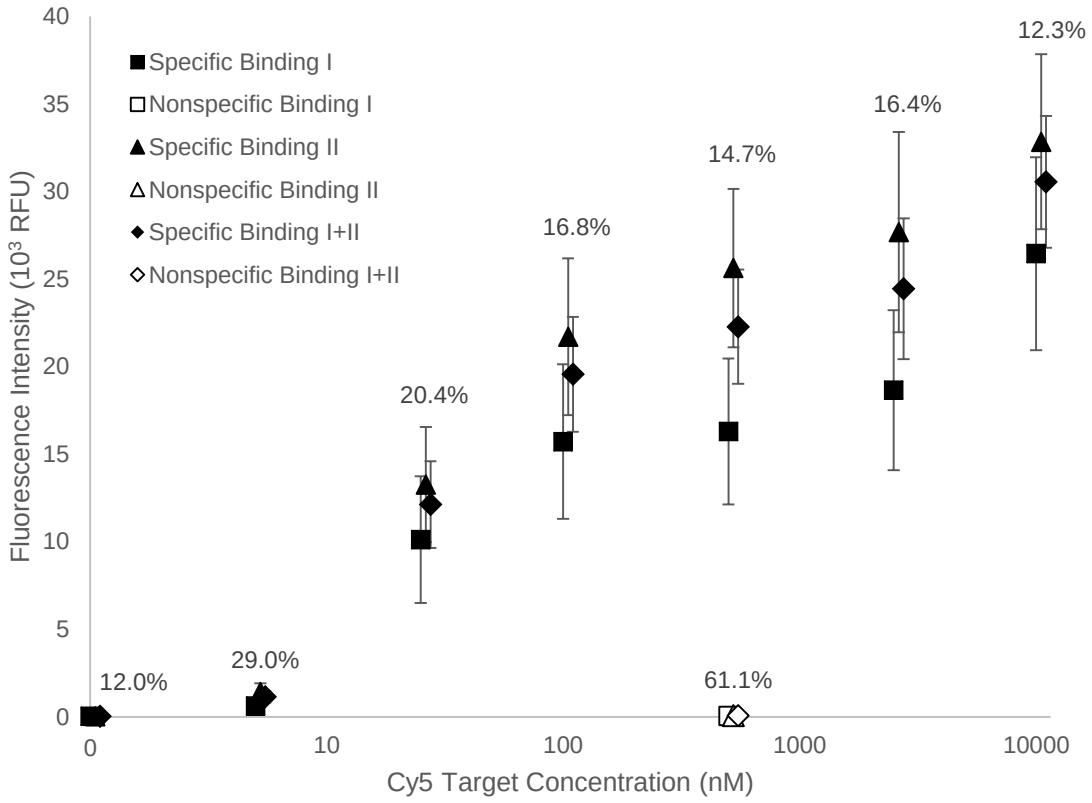

Figure 6. Results upon exposure to Cy5-DNA from two replicates using high TCEP concentrations. Slides were blocked with 20 mg/mL BSA. Wells without probe were used to obtain nonspecific binding results. Error bars indicate standard deviations from wells (n ≥ 3). Percentages indicate CV for the combined data set. Note that for 0 nM data, location on the x-axis is not to scale. Data are spaced slightly apart for clarity.

5.3 Native Target Capture

Once sensor slides were preloaded with 1 μM Cy5-target, those slides were exposed to the label-free DNA target for two hours. Initial results with low TCEP slides were poor, evincing both low signal and high noise compared to previous Cy5 binding experiments. To minimize any discrepancies from slow kinetics, slides were incubated

with native target overnight in subsequent experiments. The corresponding data demonstrated higher fluorescence intensity, substantially reduced noise, and the expected decrease in signal (Figure 7), thereby indicating the feasibility of competitive hybridization for detection of DNA targets. Nevertheless, these results exhibit only qualitative differences between different concentrations; upon further analysis, it is difficult to distinguish between each treatment. Moreover, reproducibility between slides was still rather poor, and fluorescent intensities in control wells were inconsistent with previous Cy5 binding measurements. Multiple experiments with minor procedural variations did little to alleviate these concerns.

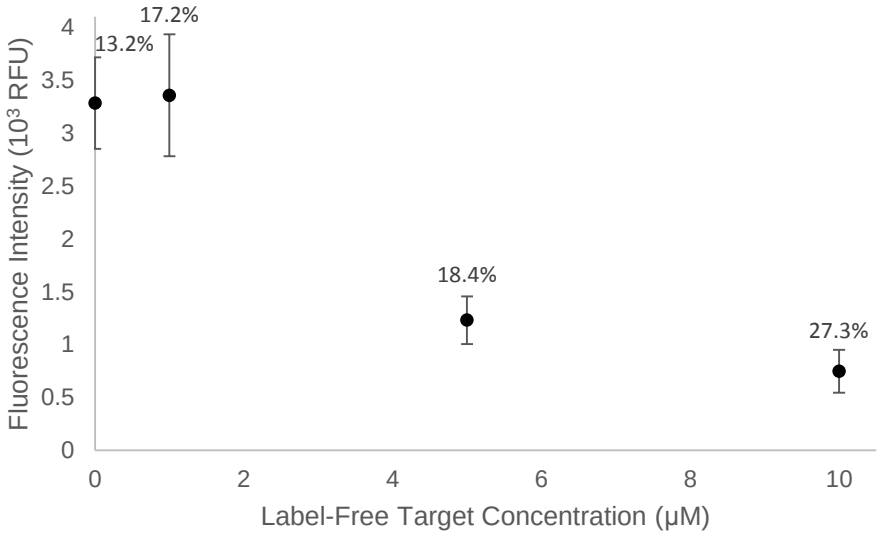

Figure 7. Preliminary results upon exposure to label-free DNA. Low TCEP concentrations were utilized for immobilization. Slides were blocked with 10 mg/mL NFDM. 1000 nM of Cy5-DNA was applied for sensor preloading. Error bars indicate standard deviations from wells (n=8). Percentages indicate CV.

Similarly, when administration of high TCEP during probe immobilization demonstrated vast improvements in Cy5-target binding, the use of high TCEP substrates was expected to remedy these continued issues with noise and reproducibility. However, when such slides (preloaded with 500 nM of Cy5-target) were exposed to native target overnight, they again evinced very low signal levels compared to corresponding Cy5-target binding curves. Furthermore, noise and reproducibility issues obscured any apparent trends within the data.

To remedy these issues, two methods were employed. First, a slide was exposed to lower amounts of native target to ensure that exposure was not exceeding the dynamic range of the sensor surface. This ameliorated the overall signal, but did little to improve noise (Figure 8). Concurrently, a slide was incubated with 2500 nM of Cy5-target to increase the signal, thereby increasing the possible contrast upon native target exposure at previous levels. Again, signal was improved, but noise remained high (Figure 9). In both cases, fluorescence trends were either not apparent or contrary to expectations. Control wells without native target also demonstrated very low signal compared to similar Cy5-target preloading studies, even at increased scanner gains.

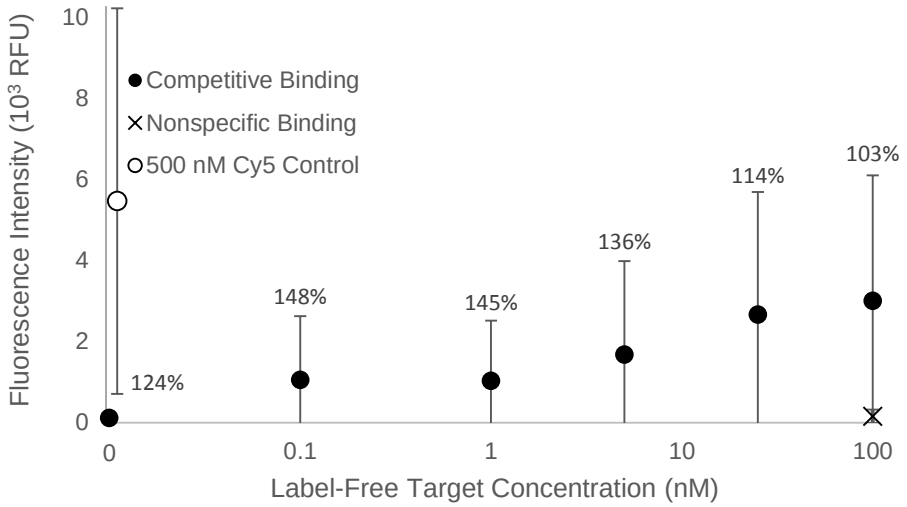

Figure 8. Results upon exposure to label-free DNA using high TCEP substrates with 500 nM of Cy5-DNA applied for sensor preloading. Wells without probe were used to obtain nonspecific binding results. Wells without competitive target were used to obtain 500 nM Cy5 control results. For comparison, the average preloading intensity at 500 nM was 22.3 ± 3.26 x 10^3 RFU (Figure 6). Error bars indicate standard deviations from wells (n=2). Percentages indicate CV for competitive binding. Note that for 0 nM data, location on the x-axis is not to scale. Data are spaced slightly apart for clarity.

These results complicate the notion of specific binding and capture implied by previous Cy5-target binding data. For some reason, competition between the native and Cy5-labelled targets occurs in a non-reproducible manner, with drastic loss of signal even without native target. One possibility is that the second series of target washes is overly stringent. In this case, excessive amounts of Cy5-target would likely become unbound simply as a result of the wash buffer strength, thereby causing a reduction of fluorescence intensity independent of the competitive binding process. This independent change would then obscure results by reducing the overall fluorescent signal even in control wells. If this

conjecture is true, a simple solution would be to employ less stringent buffers, such as PBS, for this second round of target washes in order to minimize premature loss of fluorescence.

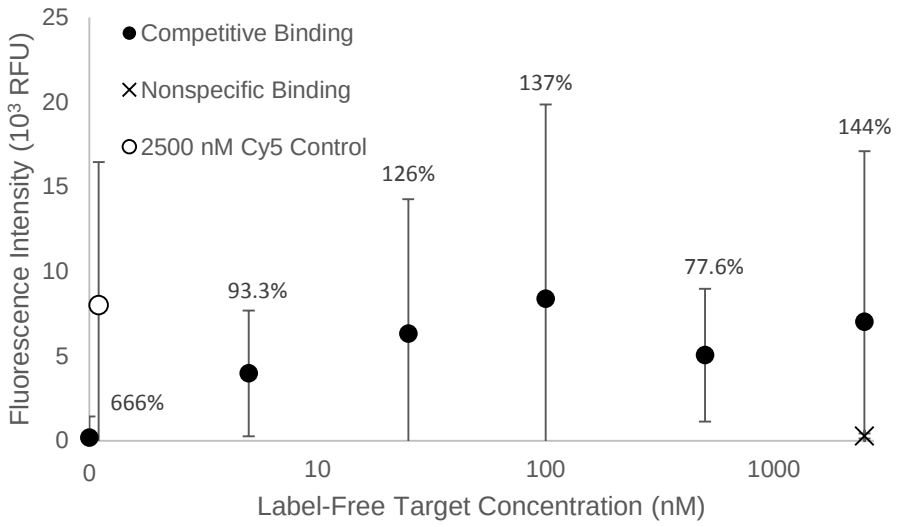

Figure 9. Results upon exposure to label-free DNA using high TCEP substrates with 2500 nM of Cy5-DNA applied for sensor preloading. Wells without probe were used to obtain nonspecific binding results. Wells without competitive target were used to obtain 2500 nM Cy5 control results. For comparison, the average preloading intensity at 2500 nM was 24.4 ± 4.02 x 10^3 RFU (Figure 6). Error bars indicate standard deviations from wells (n=2). Percentages indicate CV for competitive binding. Note that for 0 nM data, location on the x-axis is not to scale. Data are spaced slightly apart for clarity.

Alternatively, the competitive process may continue to be limited by kinetic constraints. Given that both targets have highly similar structures, the aptamer probe may be poor at distinguishing between the two at current incubation conditions, which could

reflect as high noise levels similar to those in recent results. To remedy this issue, competitive targets could be incubated with higher convection (via increased shaker speed) and at higher temperatures, thereby facilitating binding and potentially reducing the overall noise. However, this second explanation fails to account for the disparity between control wells and previous Cy5-target studies, rendering it much less likely.

A third explanation is that the silanized surface may not be stable upon prolonged exposure to aqueous media. Hydrolytic instability is a known drawback of aminosilanes, including the APTMS employed in this work.[67] If these silanes were to become unbound from the surface, they would likely be washed away, along with any bound probes and fluorescent targets. Given that the competitive binding process occurs after the surface has been exposed to aqueous media for prolonged periods, this phenomenon could explain a general loss of fluorescent signal and increased noise reflected in recent data. Precluding such issues would likely require use of an alternative silane with higher stability or higher control over surface structure via vapor-phase silanization.

6. CONCLUSIONS AND FUTURE WORK

Overall, this research has demonstrated the feasibility of an aptamer-based sensing surface for BPA detection via analogous DNA hybridization interactions. Although probe immobilization data has been inconclusive, subsequent fluorescent target studies indicate reproducible capture of those targets with minimal background in the absence of probe, implying a highly specific interaction characteristic of aptamer probes. Thus, the sensor surface has demonstrated quantitative measurements of a Cy5-labelled DNA target at various concentrations. A key parameter for this process is the TCEP concentration utilized for probe immobilization. Results demonstrated a drastic improvement of both fluorescent signal and reproducibility within Cy5-target binding studies upon introducing high levels of the reducing agent. Use of a blocking agent was also paramount in minimizing fluorescence due to nonspecific binding, with bovine serum albumin chosen due to its simplicity of use and demonstrated effectiveness.

After exposure to label-free targets at certain conditions, the preloaded sensor surface has evinced drastic reduction in fluorescence consistent with competitive binding interactions between the labeled and label-free targets. However, this trend lacks reproducibility, implying a need for further optimization of the functionalization and target exposure processes before consistent, quantitative data can be achieved.

To do so, further characterization of the probe immobilization process is key. The three primary methods utilized in this work each suffered from various flaws that obfuscated subsequent quantification. For example, ellipsometry required the use of an alternative silicon substrate and yielded data highly dependent on the chosen optical

model. Another technique, XPS, could have allowed reliable quantification of results; however, these data may have been obscured by the presence of buffer salts and TCEP. Similarly, UV/Vis measurements appeared to have suffered from substantial interference from relatively high TCEP concentrations. Given the issues surrounding these techniques, a suitable alternative must be chosen for such studies. Use of a fluorescently-labelled probe in similar fashion to the Cy5-labelled target is likely the simplest route, with quantitative measurement achieved by fluorescent imaging via the microarray scanner. Alternatively, radiolabeled DNA probes could be utilized for such a task, with the downside of necessitating additional equipment and safety precautions for quantification. Either of these techniques could be utilized to validate the immobilization of probes on the surface, thereby lending weight to previously described inferences.

Once sufficient and reproducible probe immobilization is verified, optimization of the competitive binding process would need to occur. In particular, the kinetics of competitive binding as well as the washing process would likely need to be tuned to promote specific competition while minimizing fluorescence losses via other means.

Upon doing so, sensors could then be functionalized with the probe described by Jo et al. for BPA detection.[19] To achieve the high sensitivity and low-fouling character necessary for monitoring BPA in complex biological media, this would likely involve functionalization of glass microchannels produced by collaborators. Such a device could then be incorporated into a holistic point-of-care device, complete with a handheld detector as well as a blood filtration system to provide portability, minimize interference from cells, and reduce nonspecific interactions.[50] If such research succeeds, it would

drastically improve the monitoring of BPA by enabling researchers to assess populations in a fast, reliable, and portable means. This enhanced research would in turn translate into ameliorated understanding of the consequences of BPA exposure, thereby improving safety regulations and ultimately human health outcomes.

REFERENCES

1. Genuis, S. J.; Beesoon, S.; Birkholz, D.; Lobo, R. A. Human excretion of bisphenol A: blood, urine, and sweat (BUS) study. *J. Environ. Public. Health.* **2012**, *2012*, 1-10.

2. Hormann, A. M.; vom Saal, F. S.; Nagel, S. C.; Stahlhut, R. W.; Moyer, C. L.; Ellersieck, M. R.; Welshons, W. V.; Toutain, P.; Taylor, J. A. Holding thermal receipt paper and eating food after using hand sanitizer results in high serum bioactive and urine total levels of bisphenol A (BPA). *PLOS ONE* **2014**, *9*, 1-12.

3. Huang, Y. Q.; Wong, C. K. C.; Zheng, J. S.; Bouwman, H.; Barra, R.; Wahlström, B.; Neretin, L.; Wong, M. H. Bisphenol A (BPA) in China: A review of sources, environmental levels, and potential human health impacts. *Environ. Int.* **2012**, *42*, 91-99.

4. Ragavan, K. V.; Rastogi, N. K.; Thakur, M. S. Sensors and biosensors for analysis of bisphenol-A. *TrAC Trend. Anal. Chem.* **2013**, *52*, 248-260.

5. Calafat, A. M.; Ye, X.; Wong, L.; Reidy, J. A.; Needham, L. L. Exposure of the U.S. Population to Bisphenol A and 4-tertiary-Octylphenol: 2003-2004. *Environ. Health Perspect.* **2008**, *116*, 39-44.

6. Vandenberg, L. N.; Gerona, R. R.; Kannan, K.; Taylor, J. A.; van Breemen, R. B.; Dickenson, C. A.; Liao, C.; Yuan, Y.; Newbold, R. R.; Padmanabhan, V.; vom Saal, F. S.; Woodruff, T. J. A round robin approach to the analysis of bisphenol a (BPA) in human blood samples. *Environ. Health* **2014**, *13*, 1-25.

7. Peretz, J.; Vrooman, L.; Ricke, W. A.; Hunt, P. A.; Ehrlich, S.; Hauser, R.; Padmanabhan, V.; Taylor, H. S.; Swan, S. H.; VandeVoort, C. A.; Flaws, J. A. Bisphenol a and reproductive health: update of experimental and human evidence, 2007-2013. *Environ. Health Perspect.* **2014**, *122*, 775-786.

8. Lang, I. A.; Galloway, T. S.; Scarlett, A.; Henley, W. E.; Depledge, M.; Wallace, R. B.; Melzer, D. Association of urinary bisphenol A concentration with medical disorders and laboratory abnormalities in adults. *JAMA* **2008**, *300*, 1303-1310.

9. Prins, G. S.; Hu, W.; Shi, G.; Hu, D.; Majumdar, S.; Li, G.; Huang, K.; Nelles, J. L.; Ho, S.; Walker, C. L. Bisphenol A promotes human prostate stem-progenitor cell self-renewal and increases in vivo carcinogenesis in human prostate epithelium. *Endocrinology* **2014**, *155*, 805-817.

10. Vandenberg, L. N.; Maffini, M. V.; Sonnenschein, C.; Rubin, B. S.; Soto, A. M. Bisphenol-A and the great divide: a review of controversies in the field of endocrine disruption. *Endocr. Rev.* **2009**, *30*, 75-95.

11. Li, X.; Franke, A. Improvement of bisphenol A quantitation from urine by LCMS. *Anal. Bioanal. Chem.* **2015**, *407*, 3869-3874.

12. Gubala, V.; Harris, L. F.; Ricco, A. J.; Tan, M. X.; Williams, D. E. Point of Care Diagnostics: Status and Future. *Anal. Chem.* **2012**, *84*, 487-515.

13. Brennan, D.; Justice, J.; Corbett, B.; McCarthy, T.; Galvin, P. Emerging optofluidic technologies for point-of-care genetic analysis systems: a review. *Anal. Bioanal. Chem.* **2009**, *395*, 621-636.

14. Cherkouk, C.; Rebohle, L.; Howitz, S.; Skorupa, W. Microfluidic system for endocrine disrupting chemicals detection in waterish solution. *Procedia Eng.* **2011**, *25*, 1185-1188.

15. Myers, F. B.; Lee, L. P. Innovations in optical microfluidic technologies for point-of-care diagnostics. *Lab Chip* **2008**, *8*, 2015-2031.

16. Kuang, H.; Yin, H.; Liu, L.; Xu, L.; Ma, W.; Xu, C. Asymmetric Plasmonic Aptasensor for Sensitive Detection of Bisphenol A. *ACS Appl. Mater. Interfaces* **2014**, *6*, 364-369.

17. Xue, F.; Wu, J.; Chu, H.; Mei, Z.; Ye, Y.; Liu, J.; Zhang, R.; Peng, C.; Zheng, L.; Chen, W. Electrochemical aptasensor for the determination of bisphenol A in drinking water. *Microchim. Acta* **2013**, *180*, 109-115.

18. Balamurugan, S.; Obubuafo, A.; Soper, S.; Spivak, D. Surface immobilization methods for aptamer diagnostic applications. *Anal. Bioanal. Chem.* **2008**, *390*, 1009-1021.

19. Jo, M.; Ahn, J.; Lee, J.; Lee, S.; Hong, S. W.; Yoo, J.; Kang, J.; Dua, P.; Lee, D.; Hong, S.; Kim, S. Development of Single-Stranded DNA Aptamers for Specific Bisphenol A Detection. *Oligonucleotides* **2011**, *21*, 85-91.

20. Zhu, Y.; Zhou, C.; Yan, X.; Yan, Y.; Wang, Q. Aptamer-functionalized nanoporous gold film for high-performance direct electrochemical detection of bisphenol A in human serum. *Anal. Chim. Acta* **2015**, *883*, 81-89.

21. Chung, E.; Jeon, J.; Yu, J.; Lee, C.; Choo, J. Surface-enhanced Raman scattering aptasensor for ultrasensitive trace analysis of bisphenol A. *Biosens. Bioelectron.* **2015**, *64*, 560-565.

22. Brault, N. D.; White, A. D.; Taylor, A. D.; Yu, Q.; Jiang, S. Directly functionalizable surface platform for protein arrays in undiluted human blood plasma. *Anal. Chem.* **2013**, *85*, 1447-1453.

23. Wang, L.; Li, P. C. H. Microfluidic DNA microarray analysis: A review. *Anal. Chim. Acta* **2011**, *687*, 12-27.

24. Glass, N. R.; Tjeung, R.; Chan, P.; Yeo, L. Y.; Friend, J. R. Organosilane deposition for microfluidic applications. *Biomicrofluidics* **2011**, *5*, 1-7.

25. Pujari, S. P.; Scheres, L.; Marcelis, A. T. M.; Zuilhof, H. Covalent Surface Modification of Oxide Surfaces. *Angew. Chem. Int. Edit.* **2014**, *53*, 6322-6356.

26. Cras, J. J.; Rowe-Taitt, C. A.; Nivens, D. A.; Ligler, F. S. Comparison of chemical cleaning methods of glass in preparation for silanization. *Biosens. Bioelectron.* **1999**, *14*, 683-688.

27. Shircliff, R. A.; Stradins, P.; Moutinho, H.; Fennell, J.; Ghirardi, M. L.; Cowley, S. W.; Branz, H. M.; Martin, I. T. Angle-resolved XPS analysis and characterization of monolayer and multilayer silane films for DNA coupling to silica. *Langmuir* **2013**, *29*, 4057-4067.

28. Metwalli, E.; Haines, D.; Becker, O.; Conzone, S.; Pantano, C. Surface characterizations of mono-, di-, and tri-aminosilane treated glass substrates. *J. Colloid Interface Sci.* **2006**, *298*, 825-831.

29. Howarter, J. A.; Youngblood, J. P. Optimization of silica silanization by 3-aminopropyltriethoxysilane. *Langmuir* **2006**, *22*, 11142-11147.

30. Kim, D.; Herr, A. E. Protein immobilization techniques for microfluidic assays. *Biomicrofluidics* **2013**, *7*, 1-47.

31. Witt, M.; Walter, J.; Stahl, F. Aptamer Microarrays—Current Status and Future Prospects. *Microarrays* **2015**, *4*, 115-132.

32. Hermanson, G. T. *Bioconjugate techniques;* Academic Press: 2013; pp 1165.

33. Ngundi, M. M.; Taitt, C. R.; McMurry, S. A.; Kahne, D.; Ligler, F. S. Detection of bacterial toxins with monosaccharide arrays. *Biosens. Bioelectron.* **2006**, *21*, 1195-1201.

34. Ravan, H.; Kashanian, S.; Sanadgol, N.; Badoei-Dalfard, A.; Karami, Z. Strategies for optimizing DNA hybridization on surfaces. *Anal. Biochem.* **2014**, *444*, 41-46.

35. Walter, J.; Kökpinar, O.; Friehs, K.; Stahl, F.; Scheper, T. Systematic Investigation of Optimal Aptamer Immobilization for Protein−Microarray Applications. *Anal. Chem.* **2008**, *80*, 7372-7378.

36. Raoof, M.; Jans, K.; Bryce, G.; Ebrahim, S.; Lagae, L.; Witvrouw, A. Improving the selectivity by using different blocking agents in DNA hybridization assays for SiGe bio-molecular sensors. *Microelectronic Eng.* **2013**, *111*, 421-424.

37. Deisingh, A. K.; Guiseppi-Wilson, A.; Guiseppi-Elie, A. Biochip platforms for DNA diagnostics. In *Microarrays: Preparation, Microfluidics, Detection Methods, and Biological Applications.*; Dill, K., Liu, R. H. and Grodzinski, P., Eds.; Springer: 2009; pp 271-297.

38. Guiseppi-Elie, A.; Lingerfelt, L. Impedimetric detection of dna hybridization: Towards near-patient dna diagnostics. In *Immobilisation of DNA on Chips I*; Wittmann, C., Ed.; Springer: 2005; pp 161-186.

39. Lee, C.; Harbers, G. M.; Grainger, D. W.; Gamble, L. J.; Castner, D. G. Fluorescence, XPS, and TOF-SIMS surface chemical state image analysis of DNA microarrays. *J. Am. Chem. Soc.* **2007**, *129*, 9429-9438.

40. Elhadj, S.; Singh, G.; Saraf, R. F. Optical Properties of an Immobilized DNA Monolayer from 255 to 700 nm. *Langmuir* **2004**, *20*, 5539-5543.

41. PerkinElmer. Phosphorus-32 Handling Precautions. *http://www.perkinelmer.com/CMSResources/Images/44-73994TCH_Phosphorus32.pdf* (accessed August, 2015).

42. Kingshott, P.; Andersson, G.; McArthur, S. L.; Griesser, H. J. Surface modification and chemical surface analysis of biomaterials. *Curr. Opin. Chem. Biol.* **2011**, *15*, 667-676.

43. Graf, N.; Gross, T.; Wirth, T.; Weigel, W.; Unger, W. E. Application of XPS and ToF-SIMS for surface chemical analysis of DNA microarrays and their substrates. *Anal. Bioanal. Chem.* **2009**, *393*, 1907-1912.

44. Choi, S.; Chae, J. Methods of reducing non-specific adsorption in microfluidic biosensors. *J. Micromech. Microengineering* **2010**, *20*, 075015.

45. Gong, P.; Grainger, D. Nonfouling Surfaces. In *Microarrays*; Rampal, J., Ed.; Springer: 2007; Vol. 1, pp 59-92.

46. Yu, Q.; Zhang, Y.; Wang, H.; Brash, J.; Chen, H. Anti-fouling bioactive surfaces. *Acta Biomater.* **2011**, *7*, 1550-1557.

47. Riedel, T.; Riedelová-Reicheltová, Z.; Májek, P.; Rodriguez-Emmenegger, C.; Houska, M.; Dyr, J. E.; Brynda, E. Complete identification of proteins responsible

for human blood plasma fouling on poly (ethylene glycol)-based surfaces. *Langmuir* **2013**, *29*, 3388-3397.

48. Blaszykowski, C.; Sheikh, S.; Thompson, M. Surface chemistry to minimize fouling from blood-based fluids. *Chem. Soc. Rev.* **2012**, *41*, 5599-5612.

49. Liu, B.; Wu, T.; Yang, X.; Wang, Z.; Du, Y. Portable Microfluidic Chip Based Surface-Enhanced Raman Spectroscopy Sensor for Crystal Violet. *Anal. Lett.* **2014**, *47*, 2682-2690.

50. Bunyakul, N.; Baeumner, A. J. Combining Electrochemical Sensors with Miniaturized Sample Preparation for Rapid Detection in Clinical Samples. *Sensors* **2014**, *15*, 547-564.

51. Gibbs, J. *Effective blocking procedures: ELISA Technical Bulletin - No. 3;* Corning Incorporated: Kennebunk, ME, 2001; Vol. 3, pp 6.

52. Reimhult, K.; Petersson, K.; Krozer, A. QCM-D analysis of the performance of blocking agents on gold and polystyrene surfaces. *Langmuir* **2008**, *24*, 8695-8700.

53. Gruber, H. J.; Hahn, C. D.; Kada, G.; Riener, C. K.; Harms, G. S.; Ahrer, W.; Dax, T. G.; Knaus, H. Anomalous Fluorescence Enhancement of Cy3 and Cy3.5 versus Anomalous Fluorescence Loss of Cy5 and Cy7 upon Covalent Linking to IgG and Noncovalent Binding to Avidin. *Bioconjugate Chem.* **2000**, *11*, 696-704.

54. Shen, W.; Li, S.; Park, M.; Zhang, Z.; Cheng, Z.; Petrenko, V. A.; Chin, B. A. Blocking Agent Optimization for Nonspecific Binding on Phage Based Magnetoelastic Biosensors. *J. Electrochem. Soc.* **2012**, *159*, B818-B823.

55. Taylor, S.; Smith, S.; Windle, B.; Guiseppi-Elie, A. Impact of surface chemistry and blocking strategies on DNA microarrays. *Nucleic Acids Res.* **2003**, *31*, e87.

56. Jeyachandran, Y. L.; Mielczarski, J. A.; Mielczarski, E.; Rai, B. Efficiency of blocking of non-specific interaction of different proteins by BSA adsorbed on hydrophobic and hydrophilic surfaces. *J. Colloid Interface Sci.* **2010**, *341*, 136-142.

57. Rodriguez-Emmenegger, C.; Brynda, E.; Riedel, T.; Houska, M.; Šubr, V.; Alles, A. B.; Hasan, E.; Gautrot, J. E.; Huck, W. T. Polymer Brushes Showing Non-Fouling in Blood Plasma Challenge the Currently Accepted Design of Protein Resistant Surfaces. *Macromol. Rapid Comm.* **2011**, *32*, 952-957.

58. Liu, X.; Yuan, L.; Li, D.; Tang, Z.; Wang, Y.; Chen, G.; Chen, H.; Brash, J. L. Blood compatible materials: state of the art. *J. Mater. Chem. B* **2014**, *2*, 5718-5738.

59. Sharma, S.; Popat, K. C.; Desai, T. A. Controlling nonspecific protein interactions in silicon biomicrosystems with nanostructured poly (ethylene glycol) films. *Langmuir* **2002**, *18*, 8728-8731.

60. Frederix, F.; Bonroy, K.; Laureyn, W.; Reekmans, G.; Campitelli, A.; Dehaen, W.; Maes, G. Enhanced performance of an affinity biosensor interface based on mixed self-assembled monolayers of thiols on gold. *Langmuir* **2003**, *19*, 4351-4357.

61. Brault, N. D.; Sundaram, H. S.; Li, Y.; Huang, C.; Yu, Q.; Jiang, S. Dry film refractive index as an important parameter for ultra-low fouling surface coatings. *Biomacromolecules* **2012**, *13*, 589-593.

62. de los Santos Pereira, Andres; Rodriguez-Emmenegger, C.; Surman, F.; Riedel, T.; Alles, A. B.; Brynda, E. Use of pooled blood plasmas in the assessment of fouling resistance. *RSC Adv.* **2014**, *4*, 2318-2321.

63. Gibbs, J. *Optimizing the Separation Step on 96 Well Plates: ELISA Technical Bulletin - No. 4;* Corning Incorporated: Kennebunk, ME, 2001; Vol. 4, pp 5.

64. Zhou, Q.; Liu, Y.; Shin, D.; Silangcruz, J.; Tuleuova, N.; Revzin, A. Aptamer-Containing Surfaces for Selective Capture of CD4 Expressing Cells. *Langmuir* **2012**, *28*, 12544-12549.

65. Arpat, B.; Sickler, B.; Hendrix, B. Hybridization of Cy3/5 Labeled Probes on Oligo Microarray Chips. *University of Arkansas* (accessed November, 2013).

66. Saprigin, A. V.; Thomas, C. W.; Dulcey, C. S.; Patterson, C. H.; Spector, M. S. Spectroscopic quantification of covalently immobilized oligonucleotides. *Surf. Interface Anal.* **2005**, *37*, 24-32.

67. Zhu, M.; Lerum, M. Z.; Chen, W. How to prepare reproducible, homogeneous, and hydrolytically stable aminosilane-derived layers on silica. *Langmuir* **2011**, *28*, 416-423.

68. Grody, W. W.; Nakamura, R. M.; Kiechle, F. L.; Strom, C. *Molecular diagnostics: techniques and applications for the clinical laboratory;* Academic Press: 2009; pp 484.

APPENDIX

A.1 Buffer Compositions

Phosphate buffered saline (PBS) was created by mixing 0.0136 g KH_2PO_4, 0.0804 g $Na_2HPO_4 \cdot 7(H_20)$, and 0.8775 g NaCl in 100 mL of ultrapure water. To obtain PBS+ buffer, 0.1017 g $MgCl_2 \cdot 6(H_20)$ and approximately 1 mL of Tween 20 were also added to this solution. The buffer solution was then stirred for several minutes using a magnetic stir bar until fully dissolved. Afterwards, pH was monitored using a pH meter and adjusted to approximately 7.4 using dilute solutions of NaOH and HCl. The buffer solution was stirred after each adjustment to ensure uniform properties. Initially, the buffer was then stored at room temperature; however, after repeated issues with microbial growth, buffer was instead stored in the refrigerator to prolong shelf life.

Similarly, 20x SSPE hybridization buffer was produced by adding 7.012 g NaCl and 1.104 g $Na_2HPO_4 \cdot 7(H_20)$ to 20.2 mL of 0.05 M EDTA. This solution was then brought to 32 mL using ultrapure water. Next, approximately 0.432 g NaOH (2-3 pellets) were introduced to roughly neutralize the pH. Afterwards, the solution was stirred with a magnetic stir bar until fully dissolved. The solution was then adjusted to pH 7.4 using dilute NaOH, HCl, and the pH meter. Stirring occurred after each change to ensure a homogenous solution. Once complete, the buffer volume was brought to 40 mL using ultrapure water and stored in the refrigerator until use.

20x SSC buffer was generated by mixing 0.882 g sodium citrate dihydrate and 1.735 g NaCl in 10 mL of ultrapure water. This solution was stirred using a magnetic stir bar, adjusted to pH 7.0, and stored in the refrigerator as with PBS.

A.2 Stock Reagent Compositions

$SM(PEG)_2$ was dissolved in DMSO to create a 250 mM solution. For larger quantities, $SM(PEG)_2$ was instead partitioned into aliquots at either 250 or 500 mM. Oligonucleotides were purchased from IDT or Eurofins and resuspended according to Table A.1.

Table A.1. Sequence, manufacturer, modifications, molecular weight, and resuspension buffer of various oligos. * indicates an average from both sources.

Name	Sequence
Cy5-Target	CCTCATGCCTTCTCCTCCGT
Native Target	CCTCATGCCTTCTCCTCCGT
Cy5-Probe	ACGGAGGAGAAGGCATGAGGGTGTGGCATGCGTTTTTT
Probe	ACGGAGGAGAAGGCATGAGGGTGTGGCATGCGTTTTTTTTTTTTTTTT

Name	Manufacturer	5' Mod	3' Mod	MW	Buffer
Cy5-Target	Eurofins, IDT		Cy5	6690.4 ± 125.5*	PBS
Native Target	IDT			5930.9	PBS
Cy5-Probe	Eurofins	Cy5	Disulfide	12686.8	PBS+
Probe	IDT		Disulfide	15196	PBS+

A.3 Fluorescent Image Analysis

Fluorescent images obtained from the microarray scanner were analyzed with ImageJ software. To do so, images were imported as a TIFF virtual stack. Extraneous slices from other fluorescent channels were deleted. These images were adjusted for

brightness and contrast using the built-in automatic function. Regions of interest (ROI) were then designated in each well. For experiments involving spotted probes, these ROI were circular and attempted to capture most of the fluorescent region at the spotting location. In the case of whole well functionalization (as occurred in most experiments), square ROI were chosen to best represent the square wells. These square ROI were adjusted to approximately 75% of the actual well area to avoid edge effects (e.g., the "coffee ring" effect and trapping of analytes in well corners).

Once ROI were selected, the mean intensities and standard deviations of each well were then measured and imported into Excel for further analysis. For statistical purposes, these data were considered as populations having an associated mean, standard deviation, and population size (ROI area). Overall mean and standard deviation for each treatment were then determined by the following equations,

$$Mean = \frac{\Sigma n_i x_i}{n}$$

$$Standard\ Deviation\ = \left(\frac{N_a}{N} y_a^2 + \frac{N_b}{N} y_b^2 + \frac{n_a n_b (x_a - x_b)^2}{nN}\right)^{1/2}$$

$$N_i = n_i^2 - n_i$$

$$N = (n_a + n_b)^2 - n_a - n_b$$

in which n_i is the number of measurements (i.e., area) in a given well, x_i is the mean of a given well, n is the total number of measurements (area) of all wells, and y_i is the standard deviation of a given well. These equations were similarly applied to other population-like data sets (e.g., those obtained by ellipsometry).

A.4 Optical Modeling for Ellipsometry

To interpret ellipsometry data, two main models were utilized. For most layers, a built-in Cauchy Film model was utilized, with results compared to literature values for similar compounds. The silicon substrate was likewise accounted for using preexisting models. Doing so enabled measurement of the silane and $SM(PEG)_2$ layer thicknesses.

For experiments after initial optimization of silanization, a Lorentz model was instead employed for characterization of the probe layer thickness. To do so, parameters adapted from Elhadj et al were inputted into the built-in Gen-Osc model (Table A.2). The underlying $SM(PEG)_2$ layer was set at a constant thickness equal to the average thickness from previous measurements on the same set of silicon wafers (6.40 nm).

Table A.2. Ellipsometry parameters for determining probe layer thicknesses.[40]

Parameter	Input
Amp1	0.5
Br1	0.184
En1	4.87
Einf	2.1